

AD-A183 364

ISOSBETIC POINT AND TEMPERATURE DEPENDENCE OF THE NU
SUB 2 + NU SUB L RA. (U) HOWARD UNIV WASHINGTON DC DEPT
OF CHEMISTRY G E WALRAFEN ET AL. 28 JUL 87 TR-26

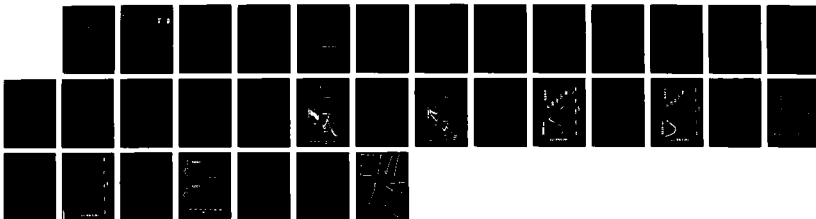
1/1

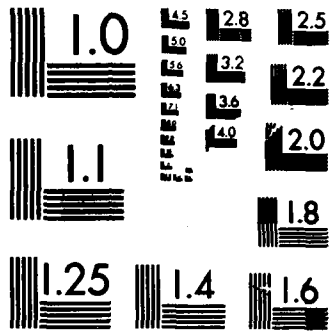
UNCLASSIFIED

NO0014-88-C-0305

F/G 7/4

NL





MICROCOPY RESOLUTION TEST CHART
NATIONAL BUREAU OF STANDARDS-1963-A

Unclassified
DTIC FILE COPY

AD-A183 364

DTIC FILE COPY

12

DOCUMENTATION PAGE

REPORT SECURITY CLASSIFICATION Unclassified		1b. RESTRICTIVE MARKINGS	
SECURITY CLASSIFICATION AUTHORITY		3. DISTRIBUTION/AVAILABILITY OF REPORT Unrestricted	
DECLASSIFICATION/DOWNGRADING SCHEDULE		5. MONITORING ORGANIZATION REPORT NUMBER DTIC SUBJECT AUG 13 1987	
PERFORMING ORGANIZATION REPORT NUMBER(S) DNR-TR-26			
NAME OF PERFORMING ORGANIZATION Howard University Department of Chemistry		7a. NAME OF MONITORING ORGANIZATION Office of Naval Research Chemistry Division	
ADDRESS (City, State, and ZIP Code) 500 College Street, NW Washington, DC 20059		7b. ADDRESS (City, State, and ZIP Code) Arlington, Virginia 22217-5000	
NAME OF FUNDING/SPONSORING ORGANIZATION		9. PROCUREMENT INSTRUMENT IDENTIFICATION NUMBER N00014-80-C-0305	
ADDRESS (City, State, and ZIP Code)		10. SOURCE OF FUNDING NUMBERS	
		PROGRAM ELEMENT NO.	PROJECT NO.
		TASK NO.	WORK UNIT ACCESSION NO.
TITLE (Include Security Classification) Isosbestic point and temperature dependence of the $\nu_2 + \nu_L$ Raman combination from liquid water.			
PERSONAL AUTHOR(S) G.E. Walrafen, M.S. Hokmabadi and W.H. Yang			
TYPE OF REPORT Technical		13b. TIME COVERED FROM TO	14. DATE OF REPORT (Year, Month, Day)
			15. PAGE COUNT 8
SUPPLEMENTARY NOTATION Submitted to Chemical Physics			
COSATI CODES		18. SUBJECT TERMS (Continue on reverse if necessary and identify by block number)	
FIELD	GROUP	SUB-GROUP	
		Water, Raman spectroscopy, Isosbestic point	
ABSTRACT (Continue on reverse if necessary and identify by block number)			
A new component has been found near 2050 cm^{-1} in the Raman spectrum of liquid water. This component refers to the two-phonon combination $\nu_2 + \nu_L$ (where ν_2 refers to intramolecular bending and L to libration), but the ν_2 and ν_L fundamental involved in this two-phonon component arise from water molecules hydrogen bonded to three rather than to four nearest neighbors. The ν_2 bending fundamental from three bonded water molecules was also uncovered. The new Raman data are in excellent agreement with published infrared data and theoretical calculations.			
DISTRIBUTION/AVAILABILITY OF ABSTRACT <input checked="" type="checkbox"/> UNCLASSIFIED/UNLIMITED <input type="checkbox"/> SAME AS RPT <input type="checkbox"/> DTIC USERS		21. ABSTRACT SECURITY CLASSIFICATION Unclassified	
NAME OF RESPONSIBLE INDIVIDUAL G. E. Walrafen		22b. TELEPHONE (Include Area Code) 202-636-6897	22c. OFFICE SYMBOL

OFFICE OF NAVAL RESEARCH

Contract N00014-80-C-805

R&T Code 4131 023

TECHNICAL REPORT NO. 26

Isosbestic Point and Temperature Dependence of the $2 + L$ Raman
Combination from Liquid Water

by

G. E. Walrafen, M. S. Hokmabadi and W. H. Yang

Submitted to Chemical Physics

Department of Chemistry
Laser Chemistry Division
Howard University
Washington, DC 20059

July 28, 1987

Reproduction in whole, or in part, is permitted for any purpose
of the United States Government.

* This document has been approved for public release and sale;
its distribution is unlimited

INTRODUCTION

A weak, broad vibrational band from liquid water whose peak occurs near 2100 cm^{-1} was previously examined by Raman [1] and infrared [2] spectroscopy. This band is structured and displays a high-frequency shoulder near 2300 cm^{-1} . It has generally been assigned as a two-phonon sum band, $\nu_2 + \nu_L$, where ν_2 refers to the intramolecular $\nu_2 A_1$ bending fundamental at 1650 cm^{-1} , and ν_L refers to one, or more, of the three intermolecular librations of water [3].

The previous infrared study involved temperatures from 5° to 75°C , [1] but the Raman investigation was conducted at room temperature. [2] Hence, it was desirable to extend the Raman work to include a similar range of temperatures, 3° to 95°C . However, other recent Raman investigations of water [4,5] involved absolute intensity measurements, and thus such absolute measurements were also carried out here. In addition, Raman measurements were performed for the depolarized and polarized geometries, X(ZX)Y and X(ZZ)Y, respectively.

The results of the new Raman investigations follow.

EXPERIMENTAL PROCEDURES

Procedures employed to obtain absolute Raman intensities were described in Refs. [4,5]. The same procedures, which involved the use of Newton's rings for cell alignment, were employed here with the J. Y. HG2S double monochromator. However, a new Raman cell was used with a much more rigorous method of water purification.

The new three-window Raman cell was constructed of brass, instead of stainless-steel [4,5]. The interior surfaces were ~~and blasted and then~~ blackened by oxidation. This procedure virtually eliminated the possibility of optical reflections from the cell walls. The in-line windows of this new cell were also placed farther apart (18 cm), which moved the blaze of the laser beam far from the vicinity of the 90-degree viewing window.

The more rigorous water purification involved distilling the water (already highly purified) directly into the Raman cell. The water was purified by two methods prior to distillation into the cell: (1) triple-distillation in an all-quartz still, and (2) passage under pressure through three columns; the first containing activated carbon, the second de-ionizing materials, and the third $0.5 \mu\text{m}$ millipore filters. The second method was

found to be preferable for removing dust.

Distillation into the Raman cell was accomplished using an all-glass entrainment line 1 meter in length. This line sloped upward at 45 degrees to the Raman cell and contained two steam traps in series. The traps and the upward slope effectively removed dust from the water. However, precautions also had to be taken to prevent dust-laden air from leaking into the Raman cell. (The Raman cell and all of its parts were washed in detergent solution and then boiled in triple-distilled water for 3 days prior to use. This procedure prevented fluorescence by removing plasticizers from the "O" rings.)

The quality of the water in the Raman cell was tested by viewing the focussed laser beam in the filled cell through the 90-degree window. After 15 consecutive distillations into the cell, one dust particle was observed to fall through a 2-cm length of the horizontal laser beam in 5 minutes. Under these conditions the green 514.5 nm Rayleigh light plus the red Raman light from the OH-stretching vibration were visually superimposed on the cell background, which was black.

A duPont 310 Curve Resolver (a special purpose analog computer) was employed for Gaussian analysis of the structured 2100 cm^{-1} contour.

RESULTS

Raman spectra corresponding to depolarized X(ZX)Y and polarized X(ZZ)Y orientations are shown for the $1000 < \bar{\nu} < 2600\text{ cm}^{-1}$ region in Figs. 1 and 2, respectively. Each figure contains two spectra, obtained at 3° and 95°C , which are comparable in terms of absolute intensities.

The following effects are evident from examination of the figures: (1) the X(ZX)Y and X(ZZ)Y spectra cross at 2060 cm^{-1} and at 2025 cm^{-1} , respectively, in the $\nu_2 + \nu_L$ combination region, (2) the $\nu_2 + \nu_L$ peak frequencies and total contour intensities decrease with increasing temperature, (3) the ν_2 bending intensity at 1650 cm^{-1} increases with temperature rise for the depolarized X(ZX)Y case, whereas just the opposite temperature dependence, i.e., a decrease in intensity, is evident for the polarized X(ZZ)Y case, and (4) the Raman intensity at 1100 cm^{-1} decreases (for both polarizations) with increase of temperature, and is larger, relative to the 1650 cm^{-1} intensity, in the X(ZZ)Y spectrum, thus indicating polarization.

The crossings evident in Figs. 1 and 2 at 3° and 95°C are shown in more detail in Figs. 3 and 4, where all of the $\nu_2 + \nu_L$ spectra of the 3° - 95°C series are shown.

From examination of Figs. 3 and 4 it is evident that the crossings of Figs. 1 and 2 are part of a more general phenomenon, namely, exact isosbestic points at 2060 cm^{-1} and 2025 cm^{-1} for the X(ZX)Y and X(ZZ)Y geometries. Other exact isosbestic points were reported recently for the OH-stretching region [4,5].

Peak frequencies obtained from the X(ZX)Y and X(ZZ)Y spectra of Figs. 3 and 4 for the $\nu_2 + \nu_L$ contour are plotted versus temperature in Fig. 5. These data are adequately represented by a linear least squares equation, and the peak frequency is seen to decrease with increasing temperature according to: $\Delta \bar{\nu}(\text{cm}^{-1}) = -0.87 t(^{\circ}\text{C}) + 2141$. Draegert et al. also observed a decrease in the $\nu_2 + \nu_L$ peak frequency in the infrared spectrum with rising temperature [2]. They reported a slope, $\Delta \nu / \Delta T$, of $-0.9 \pm 0.14 \text{ cm}^{-1}/^{\circ}\text{C}$, in excellent agreement with the present slope of $-0.87 \text{ cm}^{-1}/^{\circ}\text{C}$.

The $\nu_2 + \nu_L$ Raman contours corresponding to the X(ZX)Y and X(ZZ)Y orientation were next decomposed by means of the duPont 310 analog computer using Gaussian components. Three Gaussian components were required to obtain acceptable fits, whereas unacceptably large residuals of 10-20% resulted when only two components were used. The peak frequencies employed for the three components were: (1) $2050 \pm 10 \text{ cm}^{-1}$, (2) $2150 \pm 5-10 \text{ cm}^{-1}$, and (3) $2300 \pm 25 \text{ cm}^{-1}$. The component half-widths for the X(ZX)Y case were, respectively, 200 cm^{-1} , 250 cm^{-1} and 250 cm^{-1} . All half-widths for the X(ZZ)Y case were 200 cm^{-1} . A typical decomposition is shown in Fig. 6.

The sum of the integrated intensities of components 2 and 3, $I_2 + I_3$, was divided by the integrated intensity of component 1, I_1 , and the ratio $(I_2 + I_3)/I_1$ was plotted logarithmically versus T^{-1} . The results for the two polarizations are shown in Fig. 7.

The data of Fig. 7 were treated by linear least squares (heavy lines), i.e., $\ln[(I_2 + I_3)/I_1] = -(\Delta H^{\circ}/RT) + \text{constant}$. The X(ZX)Y and X(ZZ)Y data yielded slopes corresponding to ΔH° values of -2.4_8 and -2.4_7 kcal/mol OHO, respectively.

The error bars shown in Fig. 7 refer to analog decompositions involving both linear and curved (upwardly concave) baselines. The use of an upwardly concave baseline, as opposed to a straight baseline, however, only produced a general vertical displacement of the data, but no significant change in slope. Hence, no change in the ΔH° values resulted from the two types of baselines employed, and the error bars shown do not represent the

errors in the slopes. A value of -2.5 ± 0.1 kcal/mol OHO was obtained from analysis of the individual data sets, and is considered to represent the data of Fig. 7 adequately. This value is in excellent agreement with enthalpy values presented recently, see Table II of Ref. (5).

INTERPRETATION

A. Spectral Effects.

The isosbestic points observed in the X(ZX)Y and X(ZZ)Y spectra indicate that the $\nu_2 + \nu_1$ contour contains sub-structure involving HB and NHB components [4,5]. The decrease in the peak frequency with temperature rise is also indicative of an increase in the intensity of the 2050 cm^{-1} NHB Gaussian component (as revealed by computer analysis), relative to the sum of the 2150 and 2300 cm^{-1} HB components. The concomitant decrease in the total contour intensity with temperature rise is similar to that seen previously for the ν_2 -stretching contour [5,6] and occurs when an HB component is replaced by an NHB component having a smaller molar intensity. Because the total contour intensity is a linear combination of the HB and NHB component intensities involved, a plot of the total contour intensity is not very informative and was not shown here, although such data were available.

The opposite temperature dependences of the X(ZX)Y and X(ZZ)Y spectra at 1650 cm^{-1} is a new effect. Here, the polarized HB bending component is unresolved from the more highly depolarized NHB bending component. Previously published computer analysis indicated that the component peak frequencies, that is, the peak frequencies of the two bending components, differ by only $\approx 15 \text{ cm}^{-1}$ [1]. However, the opposite temperature dependences now observed provide much more compelling evidence for two bending components than do the usual Gaussian decomposition of

spectra corresponding to a single temperature.

The mechanism which gives rise to two spectral classes of components, HB and NHB, is discussed next.

B Mechanistic Considerations.

Consider that an H₂O molecule is tetrahedrally surrounded by four nearest-neighbor H₂O molecules to which it has formed four equal (in length, angle, etc.) hydrogen bonds, one for each of its two protons, and one for each of its two lone electron pairs. Under these circumstances the point group symmetry of the central H₂O molecule is C_{2v} and its $\nu_2 A_1$ bending vibration is strongly polarized, Figs. (1) and (2), and Ref. [7]. However, the point group symmetry must decrease when one of the four hydrogen bonds is broken (e.g., severely bent and/or stretched), Refs [5,8]. (Further, a broken hydrogen bond which involves one of the protons of the central H₂O molecule is more important, for the present discussion, than the hydrogen bonds formed by the lone pair electrons, because that breakage decouples the OH stretches of the central H₂O molecule and lowers the symmetry to C_s.) The ν_2 vibration for a C_s H₂O molecule must still be polarized, of course, but now the ν_2 depolarization ratio for the C_s molecule can be different from the ν_2 depolarization ratio for the C_{2v} molecule. For example, ρ can increase, provided that it remains less than 3/4. (The depolarization ratio, ρ , is equal to $I[X(ZX)Y] / I[X(ZZ)Y]$.) Hence, hydrogen bond rupture is clearly capable of producing two unresolved ν_2 vibrations whose properties, i.e., depolarization ratios, peak frequencies, and half-widths, are different [1].

When separate 4-bonded and 3-bonded structures exist in liquid water, it is obvious that the polarized ν_{2A_1} HB bend will only couple strongly with its corresponding 4-bonded HB librations, or which there are three. The more highly depolarized (but still polarized) $\nu_{2A'}$ bend (the prime refers to the plane of the C_s H_2O molecule) will only couple strongly with its 3-bonded librations, again 3 in terms of degrees of freedom. (These librational bands may be unresolved.) Hence the two couplings described provide the mechanism for producing pure HB and pure NHB two-phonon combination or sum bands. Stated alternatively, one would expect to see two classes of librations, with three broad components for each class, two classes of intramolecular bends, and two classes of two-phonon combination tones, with one class referring to HB or 4-bonded interactions, and the other class to NHB, i.e., 3-bonded (or fewer), interactions. Furthermore, one would also expect to find opposite temperature dependences of the intensities of these two classes.

An important mechanism leading to the formation of 4-bonded and 3-bonded structures in liquid water has recently been proposed by Giguère and Pigeon-Gosselin [8]. In the Giguère model, an H_2O molecule is surrounded tetrahedrally by four H_2O molecules to which it is fully hydrogen bonded by linear hydrogen bonds. A partial rotation of the central H_2O molecule then occurs such that a bifurcated structure results between one proton of the central H_2O molecule and two oxygen atoms of the neighboring H_2O molecules. The $O-H-O$ angle deviates markedly

from 180° for ^{the} hydrogen bond in the bifurcated structure. The other proton is unaffected and remains hydrogen bonded. (The two hydrogen bonds involving the two lone electron pairs of the central oxygen atom could also be bent. But the strain from this bending could be relieved, e.g., by change in the sp^3 hybridization.) The bifurcated structure is considered to correspond to a shallow potential minimum between two adjoining deeper minima, and it is thought to result in equal $HO_{(2)}$ and $HO_{(3)}$ distances in the $O_{(1)}-H \begin{matrix} \cdot O_{(2)} \\ \cdot O_{(3)} \end{matrix}$ structure. The $HO_{(2)} = HO_{(3)}$ distance of this structure is 2.4Å, and this value agrees exactly with the HO distance inferred by Walrafen et al. [5], who estimated NHB O-H O distances and angles for liquid water from vibrations of vicinal surface silanol groups [5]. The O-H...O angle in the bifurcated structure may be as small as 150° [5], which is equivalent to producing a 3-bonded structure because such a small angle is equivalent to breaking the hydrogen bond.

The relevance of the Giguère model to the present data is obvious. A rotation giving rise to a bifurcated structure, with its corresponding potential minimum, would lead to a libration in which one proton of the central H_2O molecule would be in an entirely new and greatly weakened force field. Only three hydrogen bonds would restrain the rotation, as opposed to the original four. Hence, a lowering of all three librational frequencies would be expected. The model is also very relevant to the restricted translations of liquid water, i.e., to O-O stretching of hydrogen-bonded O-H...O units.

The partial covalency of σ charge transfer within, linear

hydrogen bonds, decreases when the O-H...O angle decreases below 180° [5]. Therefore, oscillations of the H atom about the equilibrium $HO_{(2)} = HO_{(3)}$ distance of the bifurcated structure would preclude the type of Raman scattering produced by the partially covalent harmonic force field of linear O-H...O units.

C. Anharmonicity, and Estimation of the 3-Bonded Librational Frequency.

A weak Raman band is evident in Figs. (1) and (2) near 1300 cm^{-1} , see also Ref. (1). The qualitative polarization of this band requires that it be reassigned (1) to the overtone of the $720\text{-}740\text{ cm}^{-1}$ HB libration. (The $720\text{-}740\text{ cm}^{-1}$ feature refers to the out-of-plane libration of B_1 symmetry. Note that $B_1 \times B_1 = A_1$, which requires the overtone to be polarized. The libration around the C_2 axis, A_2 , occurs at $425\text{-}450\text{ cm}^{-1}$. The in-plane libration occurs at 550 cm^{-1} and its species is B_2 [9].) The overtone assignment of the 1300 cm^{-1} band corresponds to an anharmonicity of about 12%, which is shown to agree with the anharmonicity of the fundamental 3-bonded libration.

The Gaussian component at 2150 cm^{-1} , component (2), adjoins component (1) at 2050 cm^{-1} . Component (2) almost certainly corresponds to the sum of the two HB fundamentals, the $\nu_2 A_1$ bend at 1650 cm^{-1} , and the B_2 libration at 550 cm^{-1} . The anharmonicity for this intramolecular-intermolecular sum combination is 2.3%. The value of 2.3% is then assumed to apply to component (1) at 2050 cm^{-1} , because of its nearness to component (2). On the basis of this assumption, component (1) must correspond to the sum of the observed frequency, 1650 cm^{-1} , plus the calculated frequency, 447 cm^{-1} . But the difference between the observed frequencies of 2050 cm^{-1} and 1650 cm^{-1} is only 400 cm^{-1} . Hence, the B_1 librational anharmonicity is 12%, in agreement with the overtone value.

Next consider that component (3), the $\nu_2 + \nu_L$ HB component at 2300 cm^{-1} arises from the sum of the 1650 cm^{-1} ${}_{-2}A_1$ and $720\text{-}740 \text{ cm}^{-1}$ B_2 fundamentals. Here, the anharmonicity is $\sim 3.5\%$. However, the difference between 2300 cm^{-1} and 1650 cm^{-1} is 650 cm^{-1} , whereas the observed librational value is $\sim 730 \text{ cm}^{-1}$, thus corresponding to 12% anharmonicity.

Finally, a similar calculation for the 2150 cm^{-1} HB component assuming that it is the sum of the 1650 cm^{-1} and 550 cm^{-1} fundamentals yields an anharmonicity of 10% for the in-plane B_2 libration.

The most important conclusion of the preceding considerations is that a frequency value of $\sim 450 \text{ cm}^{-1}$ results for the 3-bonded libration. This frequency agrees with the theoretical value of 450 cm^{-1} obtained by Curnutte and Williams [10]. Moreover, the 450 cm^{-1} 3-bonded libration almost certainly refers to the in-plane B_2 motion of an H_2O molecule restrained by a hydrogen bond to one of its protons, and by two hydrogen bonds to its two lone electron pairs.

ADDENDUM

Absolute Raman intensity measurements were conducted in the frequency region of $\sim 3725\text{--}6000\text{ cm}^{-1}$, i.e., at the high-frequency foot of the intense OH-stretching region and above. A weak, broad Raman contour was observed whose maximum intensity occurs near $4000 \pm 10\text{ cm}^{-1}$ at 3°C , cf., Ref. [1]. This intensity maximum is preceded by a minimum, or at least a region of sharp upward concavity near 3900 cm^{-1} . High-frequency asymmetry is also present extending at least to 4600 cm^{-1} .

When the temperature of the water is increased to 93°C , a filling-in of Raman intensity occurs near $3910\text{--}3930\text{ cm}^{-1}$. This effect causes the contour to appear to be broadened, and this filling-in was confirmed by Raman difference spectra. An upward frequency shift of about 50 cm^{-1} is also present in the contour maximum.

The 4000 cm^{-1} contour was previously decomposed into two Gaussian components at $3990 \pm 25\text{ cm}^{-1}$ and at $4170 \pm 50\text{ cm}^{-1}$ (1). The 3990 cm^{-1} component was assigned to the combination $\nu_1 + \nu_L$ (B_2), i.e., to $3450 + 550\text{ cm}^{-1}$, and the 4170 cm^{-1} component was assigned to $\nu_1 + \nu_L$ (B_1) or $3450 + 730\text{ cm}^{-1}$ (1). Both assignments involved HB components.

The filling-in near $3910\text{--}3930\text{ cm}^{-1}$ observed from difference spectra, indicates that a high-temperature component may exist whose frequency is about 70 cm^{-1} less than that of the Gaussian (peak) component at 3990 cm^{-1} . This component, however, cannot be assigned to the sum of the 3450 cm^{-1} HB component and the 450 cm^{-1} NHB librational component because such an assignment would not allow for anharmonicity. However, an assignment involving only NHB components is reasonable, e.g., $3620 + 450\text{ cm}^{-1}$, where the 3620 cm^{-1} component refers to NHB OH-stretching (dangling OH group) (3), and the value of 450 cm^{-1} refers to the 3-bonded or NHB libration of B_2 type.

REFERENCES

1. G. E. Walrafen and L. A. Blatz, *J. Chem. Phys.* 59, 2646 (1973).
2. D. A. Draeger, N. W. B. Stone, B. Curnutte and D. Williams, *J. Optical Soc. Amer.* 56, 64 (1966).
3. G. E. Walrafen, in *Water: A Comprehensive Treatise*, edited by F. Franks (Plenum, New York, 1972).
4. G. E. Walrafen, M. S. Hokmabadi, and W.-H. Yang, *J. Chem. Phys.* 85, 6964 (1986).
5. G. E. Walrafen, M. R. Fisher, M. S. Hokmabadi, and W.-H. Yang, *J. Chem. Phys.* 85, 6970 (1986).
6. G. E. Walrafen, *J. Chem. Phys.* 47, 114 (1967).
7. P. K. Narayanaswamy, *Proc. Indian Acad. Sci.* 27A, 311 (1948).
8. P. A. Giguère and Marie Pigeon-Gosselin, *J. Raman Spectrosc.* 17 341 (1986).
9. G. E. Walrafen, *J. Chem. Phys.* 40, 3249 (1964), and Refs. (1) and (3).
10. B. Curnutte and D. Williams, in "Structure of Water and Aqueous Solutions," edited by W. A. P. Luck (Verlag Chemie, Weinheim, 1974).

ACKNOWLEDGMENTS

This work was supported by contracts from the Office of Naval Research. Thanks are due to E. Pugh for Raman work in the region of 3725-6000 cm^{-1} .

Fig. 1. Absolute Raman spectra, depolarized, X(ZX)Y orientation, for liquid water in the region from 1000 cm^{-1} to 2500 cm^{-1} at 3° and 95°C . The intense bending peak has a larger amplitude at 95°C than at 3°C , see the upper of the two superimposed peaks at 1650 cm^{-1} . Also the 95°C spectrum crosses the 3°C spectrum at 2060 cm^{-1} (and near 1175 cm^{-1}). A filling-in of the minimum near 1850 cm^{-1} thus results with rising temperature.

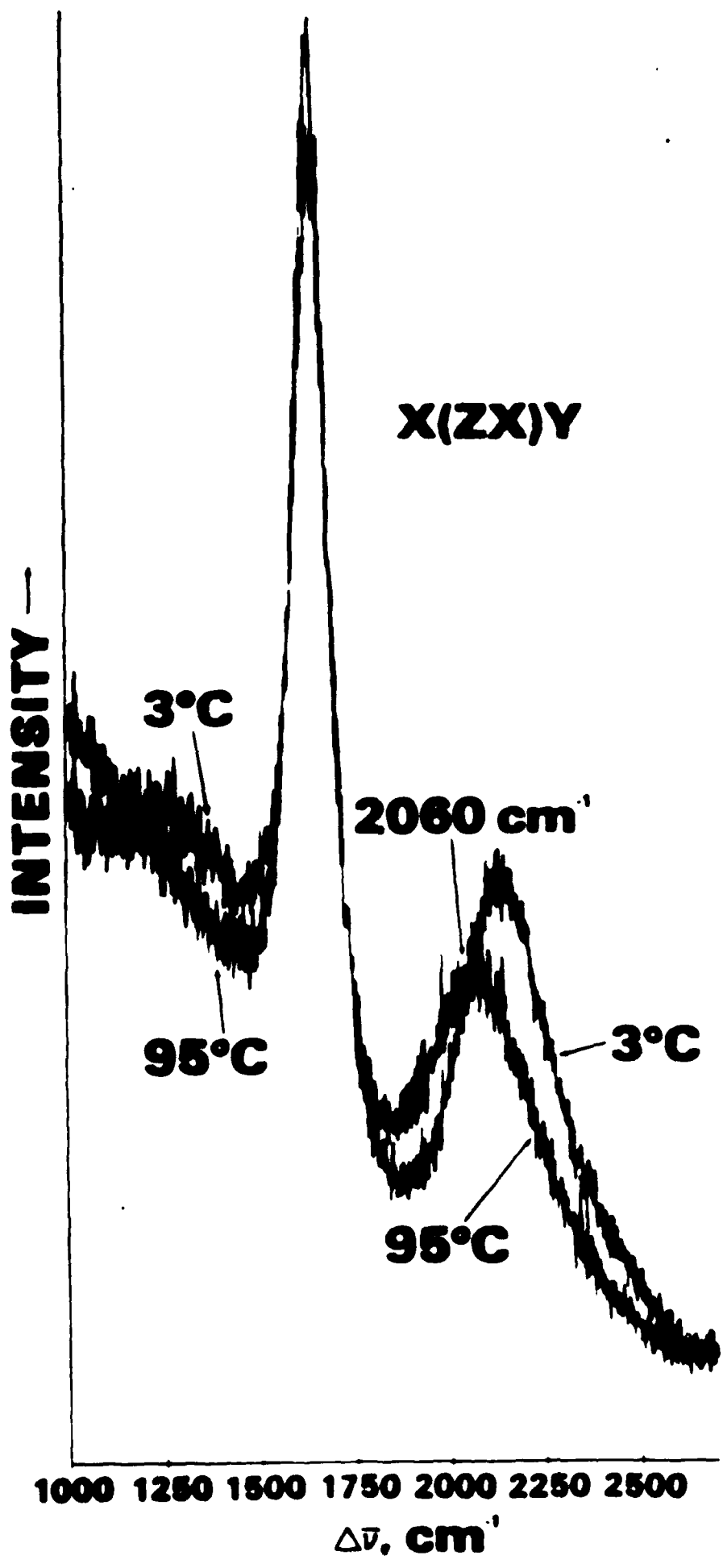


Fig. 2. Absolute Raman spectra, polarized, X(ZZ)Y orientation, for liquid water in the region from 1000 cm^{-1} to 2500 cm^{-1} at 3° and 95°C . A crossing occurs at 2025 cm^{-1} (and also near 1900 cm^{-1} , see Fig. 1). Note that the bending peak at 1650 cm^{-1} is weaker at 95°C than at 3°C for this orientation, whereas just the opposite effect occurs for the X(ZX)Y orientation, Fig. 1.

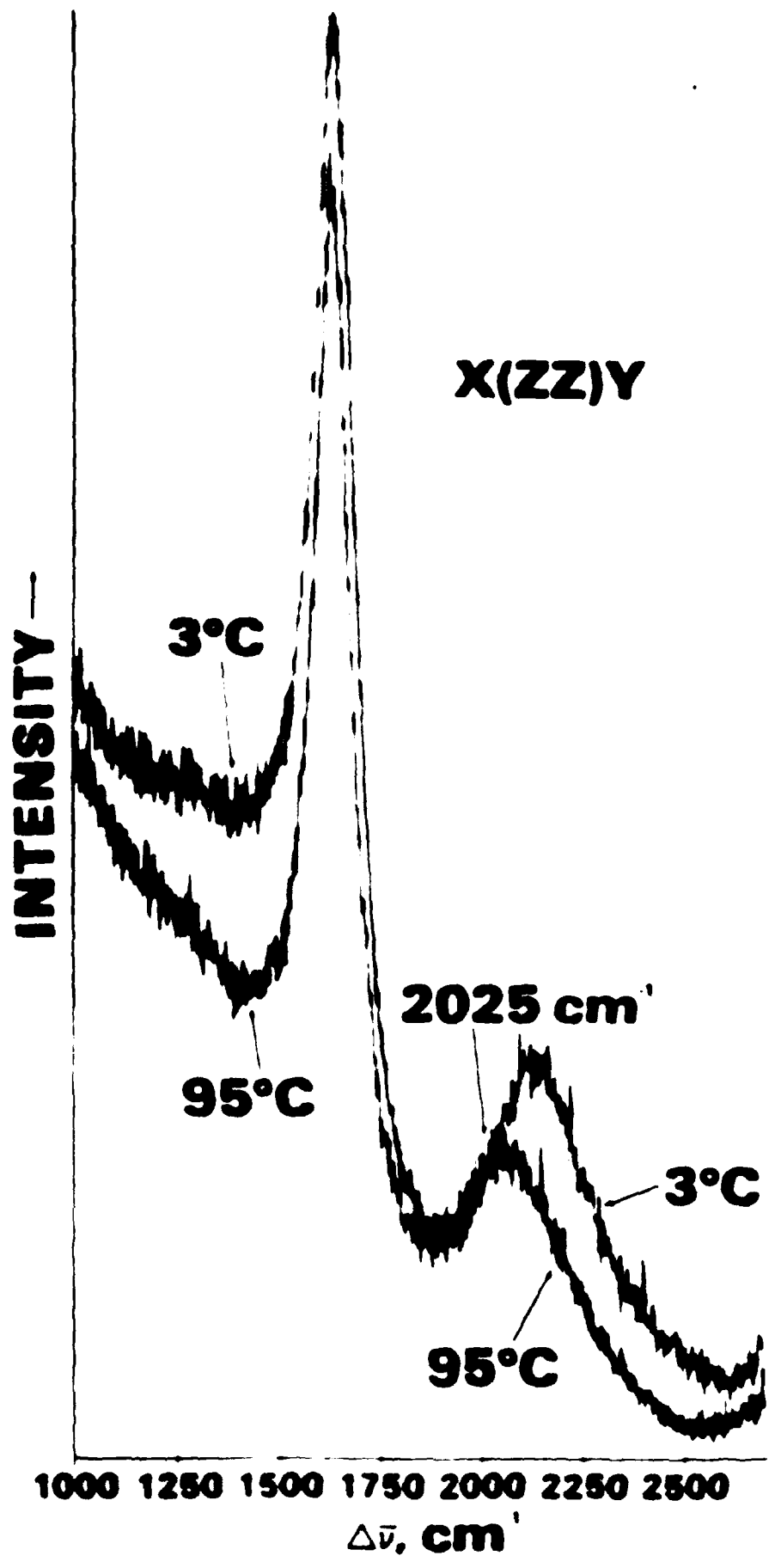


Fig. 3. Absolute Raman spectra, depolarized, X(ZX)Y orientation, for liquid water in the region from 1800 cm^{-1} to 2600 cm^{-1} for five temperatures from 3° to 95°C . Note the isosbestic point at 2060 cm^{-1} .

Fig. 3.

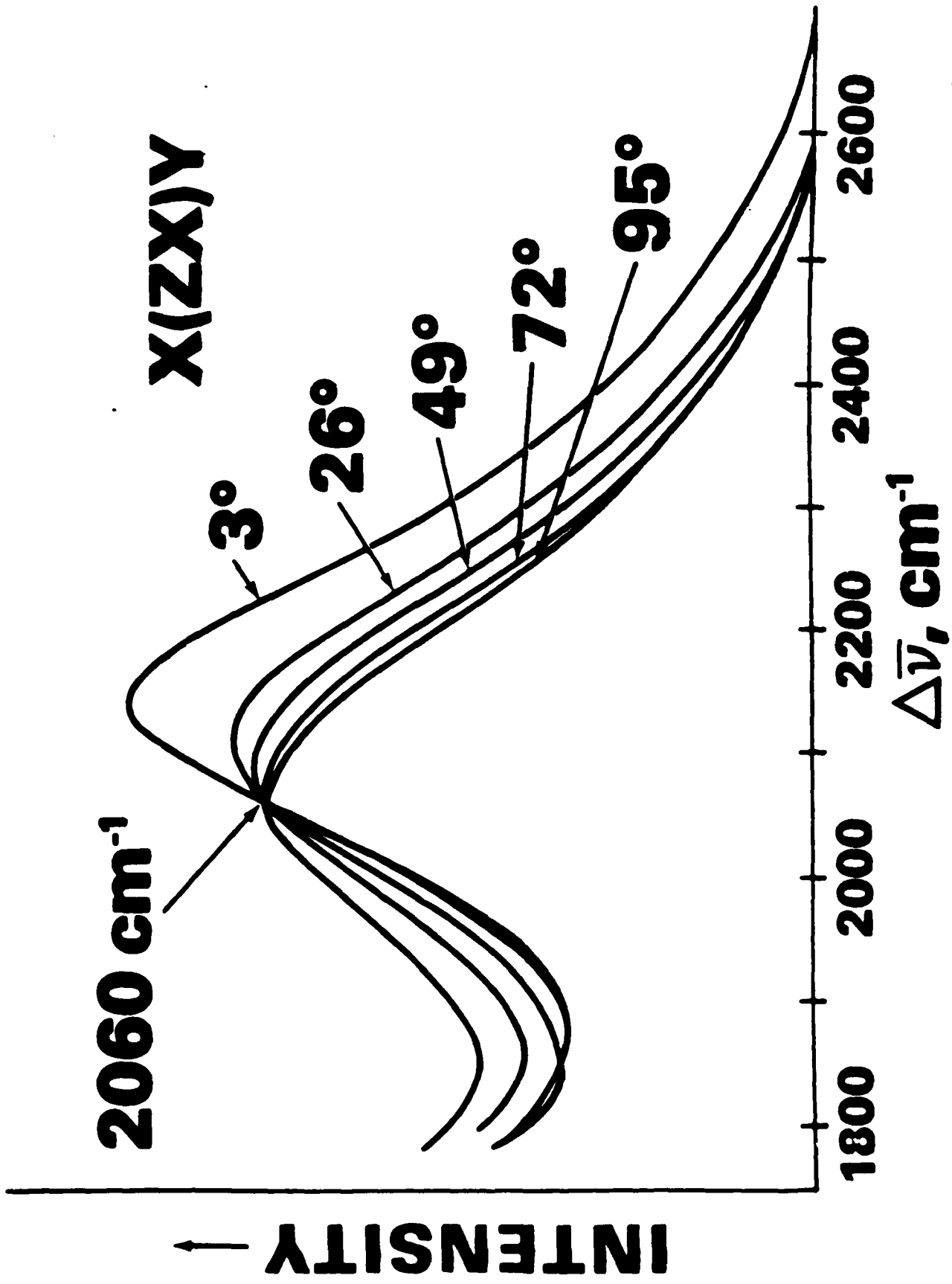


Fig. 4. Absolute Raman spectra, polarized, X(ZZ)Y orientation, for liquid water in the region from 1800 cm^{-1} to 2600 cm^{-1} for five temperatures from 3° to 95°C . An isosbestic point occurs at 2025 cm^{-1} which is 45 cm^{-1} below the X(ZX)Y isosbestic point, Fig. 3. A subsidiary point also occurs near 1900 cm^{-1} .

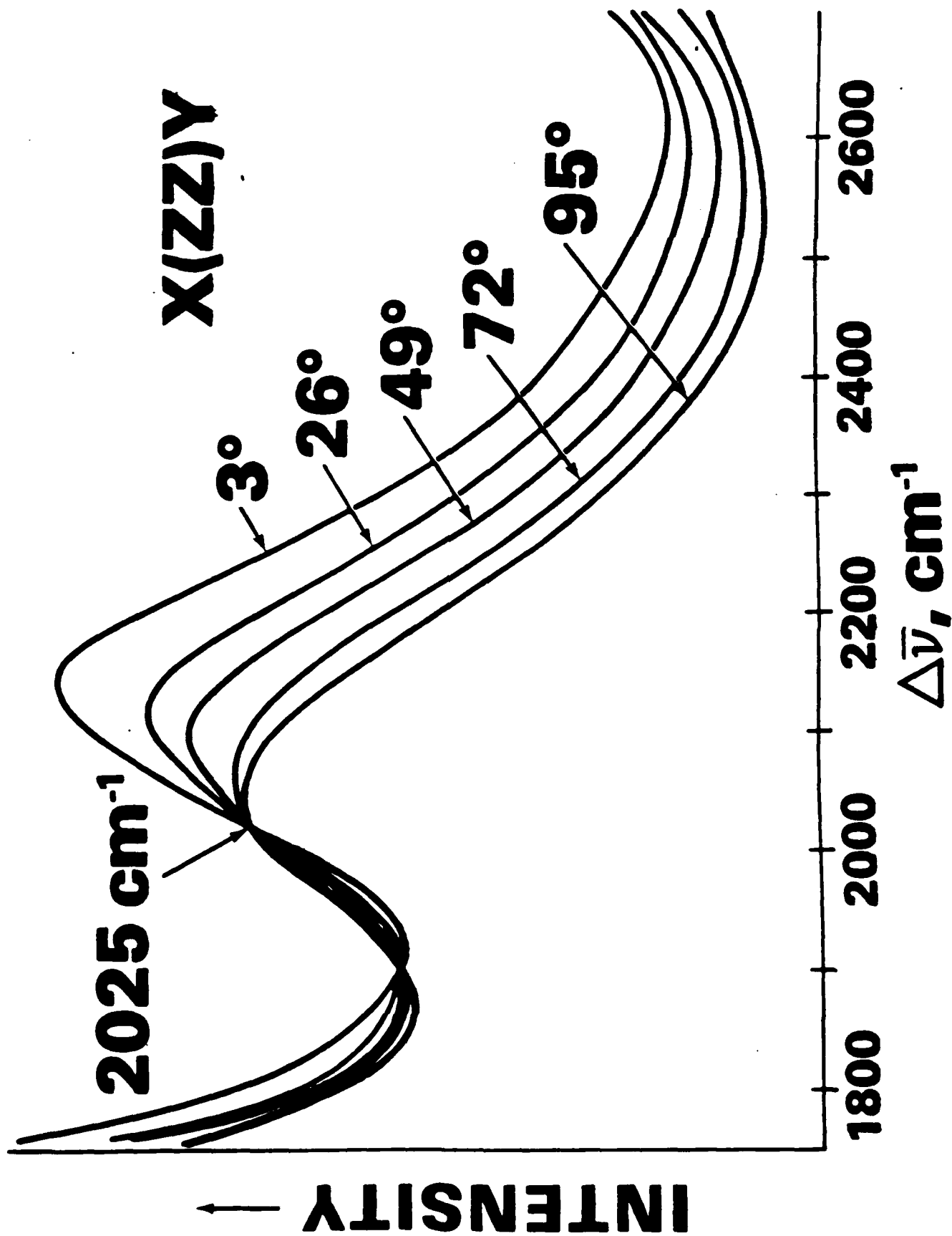


Fig. 4.

Fig. 5. Shift in the position of the peak of the two-phonon, bending plus librational Raman contour from liquid water as a function of temperature from 3° to 95°C. Least square equation shown on the figure. Diamonds, X(ZX)Y, and circles, X(ZZ)Y, orientations.

Fig. 5.

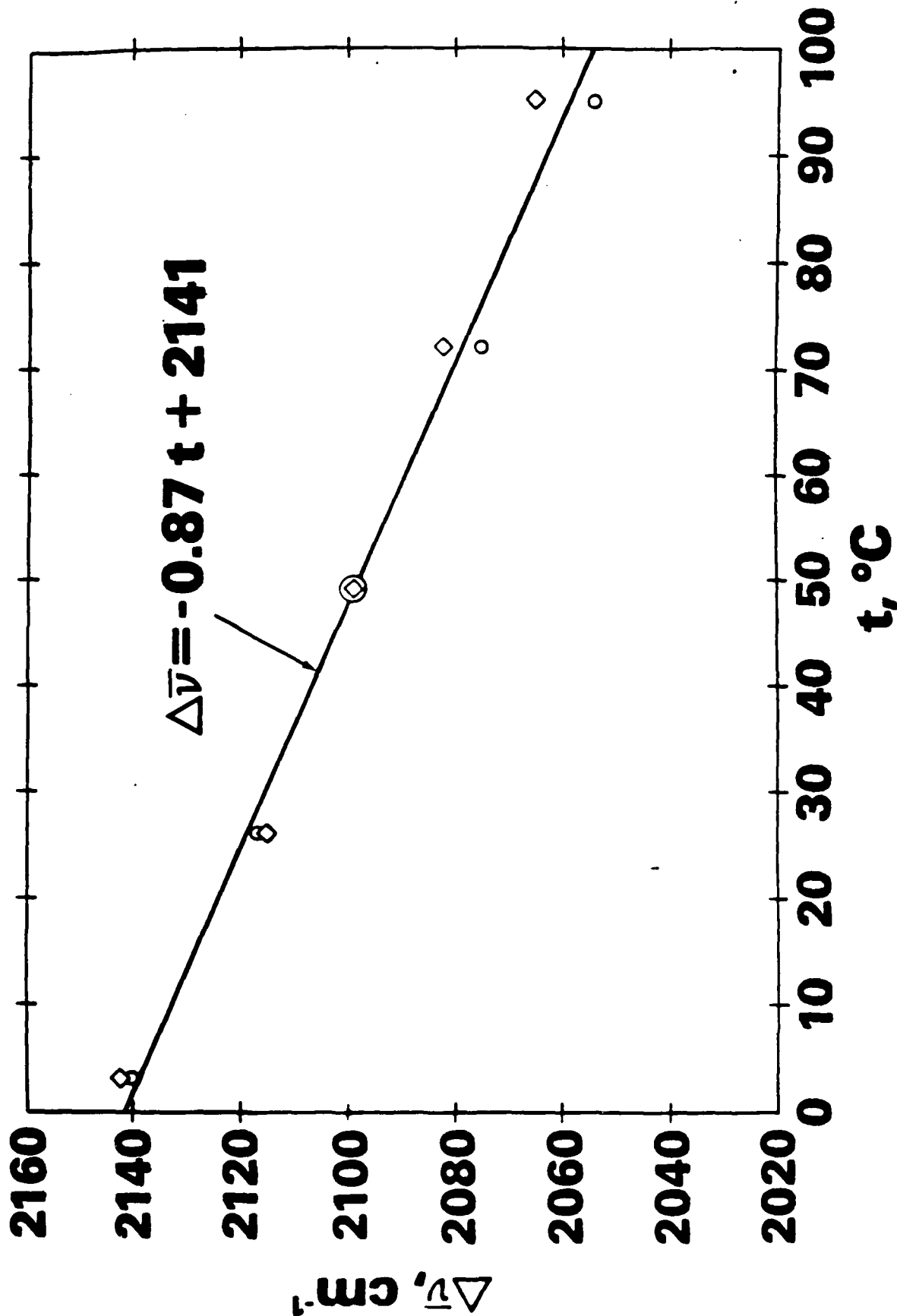


Fig. 6. Typical 3-Gaussian analysis of the two-phonon, bending plus librational Raman contour for liquid water using a baseline (dashed) which is upwardly concave. Component 1 is a NHB component whose intensity rises with increasing temperature, whereas the HB components 2 and 3, show the opposite temperature dependence. Polarized, X(ZZ)Y orientation, 49°C.

Fig. 6.

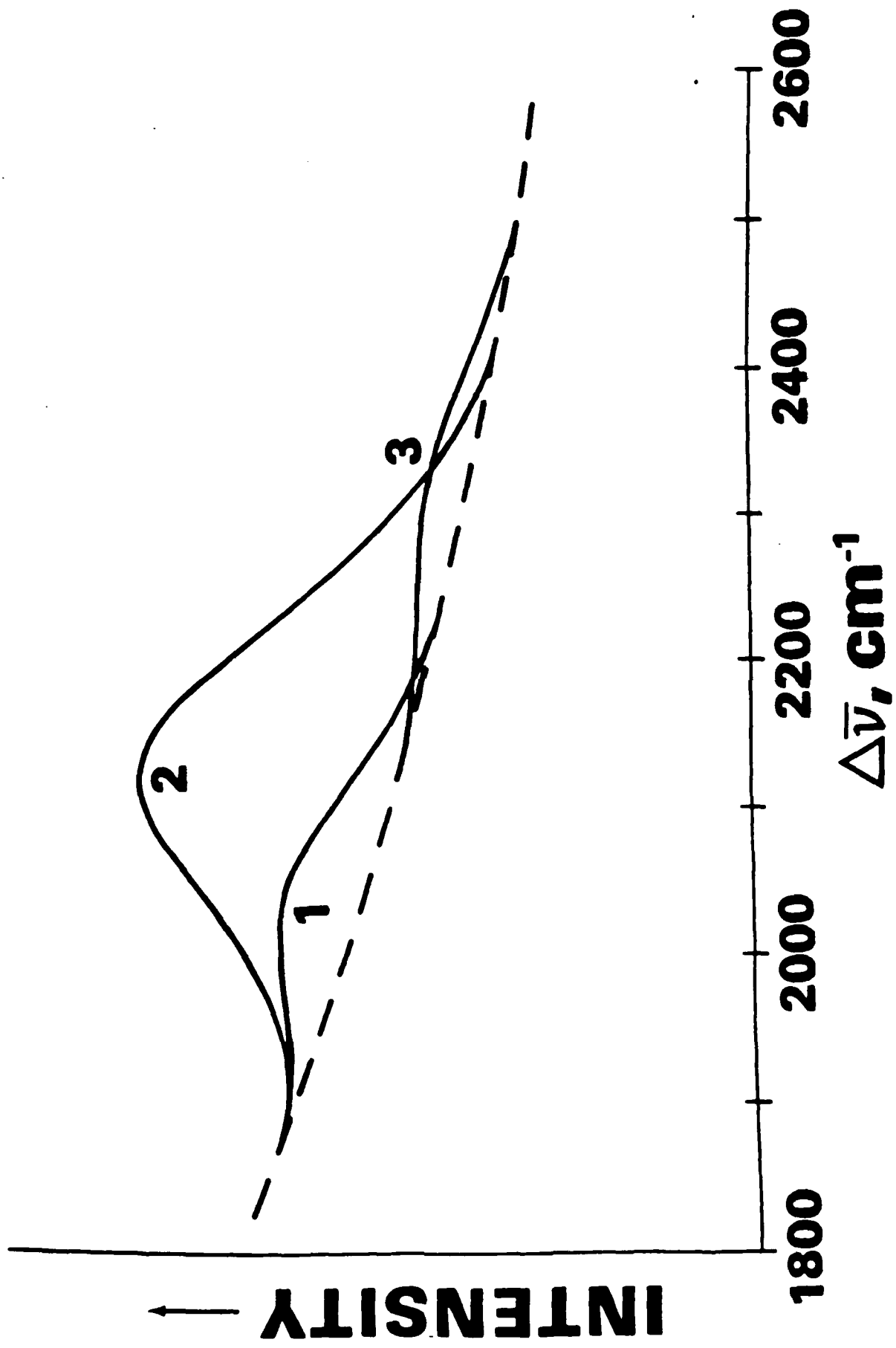
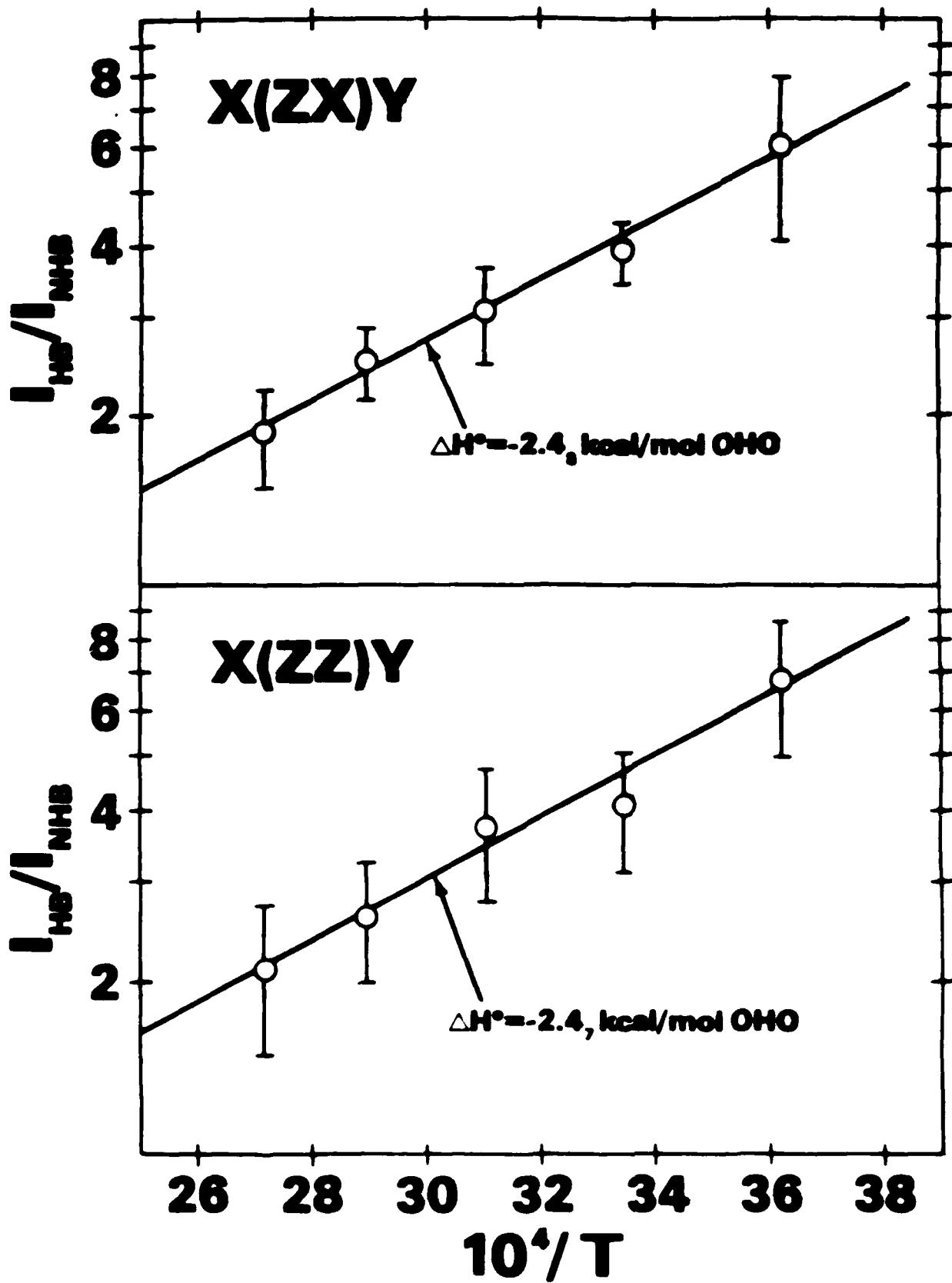


Fig. 7. The ratio I_{222}/I_{222} on a logarithmic scale versus $10^4/T$ for liquid water from 3° to 95 °C. I_{222} is the integrated Raman intensity of component 1, Fig. 6, and I_{222} is the sum of the integrated intensities of components 2 and 3. The extremes of the error bars refer to different baseline curvatures as discussed in the text. The lines shown through the data refer to least squares. The ΔH° values shown refer to the enthalpy of formation of O-H...O units.



DL/1113/87/2

TECHNICAL REPORT DISTRIBUTION LIST, GEN

	<u>No. Copies</u>		<u>No. Copies</u>
Office of Naval Research Attn: Code 1113 800 N. Quincy Street Arlington, Virginia 22217-5000	2	Dr. David Young Code 334 NORDA NSTL, Mississippi 39529	1
Dr. Bernard Doude Naval Weapons Support Center Code 50C Crane, Indiana 47522-5050	1	Naval Weapons Center Attn: Dr. Ron Atkins Chemistry Division China Lake, California 93555	1
Naval Civil Engineering Laboratory Attn: Dr. R. W. Drisko, Code L52 Port Hueneme, California 93401	1	Scientific Advisor Commandant of the Marine Corps Code RD-1 Washington, D.C. 20380	1
Defense Technical Information Center Building 5, Cameron Station Alexandria, Virginia 22314	12 high quality	U.S. Army Research Office Attn: CRD-AA-IP P.O. Box 12211 Research Triangle Park, NC 27709	1
DTNSRDC Attn: Dr. H. Singerman Applied Chemistry Division Annapolis, Maryland 21401	1	Mr. John Boyle Materials Branch Naval Ship Engineering Center Philadelphia, Pennsylvania 19112	1
Dr. William Tolles Superintendent Chemistry Division, Code 6100 Naval Research Laboratory Washington, D.C. 20375-5000	1	Naval Ocean Systems Center Attn: Dr. S. Yamamoto Marine Sciences Division San Diego, California 91232	1

ABSTRACTS DISTRIBUTION LIST, 051A

Dr. M. A. El-Sayed
Department of Chemistry
University of California
Los Angeles, California 90024

Dr. E. R. Bernstein
Department of Chemistry
Colorado State University
Fort Collins, Colorado 80521

Dr. J. R. MacDonald
Chemistry Division
Naval Research Laboratory
Code 6110
Washington, D.C. 20375-5000

Dr. G. B. Schuster
Chemistry Department
University of Illinois
Urbana, Illinois 61801

Dr. J. B. Halpern
Department of Chemistry
Howard University
Washington, D.C. 20059

Dr. M. S. Wrighton
Department of Chemistry
Massachusetts Institute of Technology
Cambridge, Massachusetts 02139

Dr. W. E. Moerner
I.B.M. Corporation
Almaden Research Center
650 Harry Rd.
San Jose, California 95120-6099

Dr. A. B. P. Lever
Department of Chemistry
York University
Downsview, Ontario
CANADA M3J1P3

Dr. George E. Walrafen
Department of Chemistry
Howard University
Washington, D.C. 20059

Dr. Joe Brandelik
AFMAL/AADO-1
Wright Patterson AFB
Fairborn, Ohio 45433

Dr. Carmen Ortiz
Consejo Superior de
Investigaciones Cientificas
Serrano 121
Madrid 6, SPAIN

Dr. Kent R. Wilson
Chemistry Department
University of California
La Jolla, California 92093

Dr. G. A. Crosby
Chemistry Department
Washington State University
Pullman, Washington 99164

Dr. Theodore Pavlopoulos
NOSC
Code 521
San Diego, California 91232

Dr. John Cooper
Code 6173
Naval Research Laboratory
Washington, D.C. 20375-5000

Dr. Joseph H. Boyer
Department of Chemistry
University of New Orleans
New Orleans, Louisiana 70148

Dr. Harry D. Gafney
Department of Chemistry
Queens College of CUNY
Flushing, New York 11367-0904

END

9-87

Dtic